THE JOURNAL OF BIOLOGICAL CHEMISTRY VOL. 289, NO. 43, pp. 29728–29738, October 24, 2014


# Endoplasmic Reticulum-associated Inactivation of the Hormone Jasmonoyl-L-Isoleucine by Multiple Members of the Cytochrome P450 94 Family in *Arabidopsis*[*] [S]

Received for publication, August 7, 2014, and in revised form, September 9, 2014 Published, JBC Papers in Press, September 10, 2014, DOI 10.1074/jbc.M114.603084

**Abraham J. Koo[‡§¶1,2], Caitlin Thireault[‡], Starla Zemelis[‡3], Arati N. Poudel[§¶‖2], Tong Zhang[§¶2], Naoki Kitaoka[**], Federica Brandizzi[‡3], Hideyuki Matsuura[**], and Gregg A. Howe[‡ ‡‡]**

*From the [‡]Department of Energy-Plant Research Laboratory and [‡‡]Department of Biochemistry and Molecular Biology, Michigan State University, East Lansing, Michigan 48824, [**]Division of Applied Bioscience, Research Faculty of Agriculture, Hokkaido University, Sapporo 060-8589, Japan, and [§]the Division of Biochemistry, [¶]Interdisciplinary Plant Group, and [‖]Division of Plant Sciences, University of Missouri, Columbia, Missouri 65211*

**Background:** Accumulation of the plant hormone jasmonoyl-L-isoleucine (JA-Ile) is tightly controlled to prevent overactivation of defense responses.
**Results:** Cytochrome P450 94s (CYP94s) with distinct tissue expression patterns localize to ER and oxidize JA-Ile to a dicarboxy derivative that fails to assemble JA-Ile co-receptor complexes.
**Conclusion:** Sequential CYP94-catalyzed oxidations block receptor activation and signaling.
**Significance:** P450s inactivate fatty acid-derived signals in both plants and animals.

**The plant hormone jasmonate (JA) controls diverse aspects of plant immunity, growth, and development. The amplitude and duration of JA responses are controlled in large part by the intracellular level of jasmonoyl-L-isoleucine (JA-Ile). In contrast to detailed knowledge of the JA-Ile biosynthetic pathway, little is known about enzymes involved in JA-Ile metabolism and turnover. Cytochromes P450 (CYP) 94B3 and 94C1 were recently shown to sequentially oxidize JA-Ile to hydroxy (12OH-JA-Ile) and dicarboxy (12COOH-JA-Ile) derivatives. Here, we report that a third member (CYP94B1) of the CYP94 family also participates in oxidative turnover of JA-Ile in *Arabidopsis*. *In vitro* studies showed that recombinant CYP94B1 converts JA-Ile to 12OH-JA-Ile and lesser amounts of 12COOH-JA-Ile. Consistent with this finding, metabolic and physiological characterization of *CYP94B1* loss-of-function and overexpressing plants demonstrated that CYP94B1 and CYP94B3 coordinately govern the majority (>95%) of 12-hydroxylation of JA-Ile in wounded leaves. Analysis of *CYP94-promoter-GUS* reporter lines indicated that CYP94B1 and CYP94B3 serve unique and overlapping spatio-temporal roles in JA-Ile homeostasis. Subcellular localization studies showed that CYP94s involved in conversion of JA-Ile to 12COOH-JA-Ile reside on endoplasmic reticulum (ER). *In vitro* studies further showed that 12COOH-JA-Ile, unlike JA-Ile, fails to promote assembly of COI1-JAZ co-receptor complexes. The double loss-of-function mutant of CYP94B3 and ILL6, a JA-Ile amidohydrolase, displayed a JA profile consistent with the collaborative action of the oxidative and the hydrolytic pathways in JA-Ile turnover. Collectively, our results provide an integrated view of how multiple ER-localized CYP94 and JA amidohydrolase enzymes attenuate JA signaling during stress responses.**



[*] This work was supported in part by National Institutes of Health Grant No. GM57795 (to G. A. H.) and the Chemical Sciences, Geosciences, and Biosciences Division, Office of Basic Energy Sciences, Office of Science, U. S. Department of Energy (Grant No. DE-FG02-91ER20021) for partial support of A. J. K. and C. T.
[S] This article contains supplemental Table S1.
[1] To whom correspondence should be addressed: Division of Biochemistry, University of Missouri, Columbia, MO. Tel.: 573-882-9227; Fax: 573-882-5635; E-mail: kooaj@missouri.edu.
[2] Supported by the Food for the 21st Century Program, University of Missouri (to A. J. K.).
[3] Supported by the Department of Energy (DOE) Great Lakes Bioenergy Research Center (DOE Office of Science BER DE-FC02-07ER64494) and National Science Foundation (NSF) (MCB1243792).

The fatty-acid derived plant hormone jasmonate (JA)[4] controls a wide range of chemical and morphological defense responses to arthropod herbivores, microbial pathogens and other forms of biotic stress (1, 2). JA also plays essential roles in plant growth and development, including sexual reproduction and growth regulation (3–5). Components of the core JA signaling module interact directly with many other phytohormone response pathways to mediate adaptive responses to changing environments (6, 7). Most JA responses are regulated at the transcriptional level by fluctuations in the intracellular level of the bioactive form of JA, jasmonoyl-L-isoleucine (8–10). Despite detailed knowledge of the enzymatic steps involved in the production of JA-Ile (2, 11, 12), relatively little is known about the enzymatic and cellular processes underlying other aspects of JA-Ile homeostasis, including JA transport and catabolism.

JA-Ile exerts its effects on gene expression by promoting degradation of Jasmonate ZIM-domain (JAZ) repressor proteins via the ubiquitin-proteasome system. In cells containing low levels of JA-Ile, the activity of transcription factors such as

[4] The abbreviations used are: JA, jasmonate; JAZ, Jasmonate ZIM-domain; CYP, cytochrome P450; JA-Ile, jasmonoyl-L-isoleucine; MeJA, methyl-jasmonic acid; 12OH-JA-Ile, 12-hydroxy-jasmonoyl-L-isoleucine; 12COOH-JA-Ile, 12-carboxy-jasmonoyl-isoleucine; GUS, β-glucuronidase; X-glu, β-glucuronic acid.

MYC2 that positively regulate JA-responsive genes is repressed by direct binding of JAZ proteins and associated co-repressors (13–15). Elevated JA-Ile levels promote binding of JAZ proteins to Coronatine Insensitive1 (COI1), which is the F-box protein component of the E3 ubiquitin ligase $SCF^{COI1}$ (14, 16). Proteolytic degradation of JAZ substrates via the ubiquitin-proteasome system releases MYC2 and other transcription factors from repression, thereby leading to expression of JA-response genes.

The JA signaling module is part of a complex phytohormone network that exerts exquisite control over the allocation of metabolic resources between the competing processes of growth and defense (17–19). Given the fitness costs associated with expression of JA-regulated defenses, which are energetically demanding and potentially toxic, plants appear to have evolved various strategies to attenuate the strength of these responses (20, 21). Several mechanisms to reign in JA responses have recently been elucidated (22). The rapid JA-dependent transcriptional induction of *JAZ* genes implies that *de novo* synthesized JAZ proteins exert negative feedback control (23). Alternative splicing events that remove or weaken the COI1-interacting JAZ degron provide a mechanism to produce JAZ variants that are more resistant to ubiquitin-mediated degradation, thus repressing JA responses in cells containing high JA-Ile levels (24–26). Similarly, some full-length JAZ proteins (*e.g.* JAZ8) have a non-canonical degron that does not interact with COI1 in the presence of JA-Ile (27). These JAZs therefore accumulate and repress their target transcription factors in the presence of JA-Ile. Another mechanism of negative feedback involves JA-dependent expression of negative-acting bHLH transcription factors that compete with MYC2 for *cis*-regulatory elements in the promoters of JA-responsive genes (28–31).

Superimposed upon these transcription-based mechanisms for signal attenuation is an independent negative feedback loop involving JA-induced catabolism of JA-Ile. Two major pathways for catabolic inactivation of JA-Ile have recently been described. One pathway is catalyzed by amidohydrolases that cleave JA-Ile to jasmonic acid and Ile (32–34). A second pathway involves oxidation of the C12 position JA-Ile to generate 12OH-JA-Ile, which is further oxidized to the carboxyl derivative 12COOH-JA-Ile (35–37). Elucidation of this pathway was advanced by the discovery that two members (CYP94B3 and CYP94C1) of the CYP94 family of cytochromes P450 in *Arabidopsis* catalyze the sequential oxidation reactions (38–40). 12OH-JA-Ile exhibits reduced capacity to promote formation of COI1-JAZ co-receptor complexes (38) but the activity of other oxidized derivatives of the hormone remains unknown.

Here, we report the identification and characterization of CYP94B1 as a third enzyme in the ω-oxidation pathway for JA-Ile catabolism. Our results indicate that CYP94B1 and CYP94B3 work coordinately to catalyze the initial oxidation of JA-Ile in overlapping and distinct tissues of *Arabidopsis*. We also show that sequential oxidation of JA-Ile by CYP94s occurs on endoplasmic reticulum (ER), and that the 12COOH-JA-Ile product of this pathway fails to promote the formation of COI1-JAZ co-receptor complexes. Collectively, our results provide an integrated view of how ER-localized CYP94 enzymes attenuate JA signaling during stress responses.

## EXPERIMENTAL PROCEDURES

*Plant Material, Growth, and Treatments—Arabidopsis thaliana* ecotype Col-0 was used as the wild-type (WT) for all experiments, and was grown as previously described (41). T-DNA insertion lines *cyp94b1-1* (SALK_129672) and *cyp94b1-2* (SALK_132621 were obtained from the *Arabidopsis* Biological Resource Center. Previously described (33) *ill6-1* (SALK_024894C) seed was provided by Dr. John Browse at Washington State University. A complete list of primers used in this study is provided in supplemental Table S1. *Nicotiana tabacum* (cv Petit Havana) plants used to infiltrate *Agrobacterium tumefaciens* harboring constructs for subcellular localization studies were grown in a growth chamber maintained under 18 h of light (40 $\mu$E $m^{-2}$ $s^{-1}$) at 23 °C and 6 h of dark at 18 °C.

Transgenic lines overexpressing *CYP94B3* (At3g48520) were as described previously (38). Binary vector constructs for generating *CYP94B1-OE* lines were made by PCR-amplifying the full-length *CYP94B1* (At5g63450) open reading frame (ORF) from WT genomic DNA template using the primer pair JH3_XbaI F and JH3_XhoI R1 (supplemental Table S1) and ligating the resulting PCR fragment into the XbaI and XhoI sites of a modified pBI121 vector (41), which places the gene under the control of the cauliflower mosaic virus (CaMV) $^{35}$S promoter.

Transgenic plants expressing β-glucuronidase (GUS) under the control of the respective promoters were generated for the tissue-specific expression study of *CYP94B1* and *CYP94B3*. Promoter regions 1.8 kb and 2.0 kb upstream of *CYP94B1* and *CYP94B3* translation initiation sites were PCR amplified from *Arabidopsis* (Col-0) genomic DNA using primers shown in supplemental Table S1 and were cloned in front of *uidA* gene (GUS) of pBI121 using ClaI and XmaI restriction sites.

The resulting *$^{35}$S:CYP94B1*, *CYP94B1promoter:GUS and CYP94B3promoter:GUS* constructs were transformed first into *A. tumefaciens* strain C58C1 then to *Arabidopsis* by the floral dip method. T1 seeds were first screened for their antibiotic resistance on Murashige and Skoog (MS) medium containing kanamycin (50 $\mu$g $ml^{-1}$) and vancomycin (100 $\mu$g $ml^{-1}$), and upon transfer to soil, 20 lines harboring *$^{35}$S:CYP94B1* (*CYP94B1-OE*) were analyzed for mRNA expression of the transgene, jasmonate profile, and fertility. Among these, three *CYP94B1-OE* lines were propagated to obtain homozygous T3 lines. *CYP94B1promoter:GUS* (*B1pro:GUS*) and *CYP94B3promoter:GUS* (*B3pro:GUS*) lines were selected by staining 20 ~ 24-d old rosette leaves for GUS activity after either treating with methyl jasmonate (MeJA) or mechanically wounding for 24 h. For MeJA treatment, ten microliter of 50 $\mu$M MeJA was spotted onto a leaf surface divided into 4~6 droplets. For wounding, one leaf per plant was crushed twice across the midrib with a hemostat. MeJA treated or wounded leaves were collected after 24 h of treatment for histochemical GUS staining. Control untreated leaves were collected prior to MeJA or wounding treatment. Wounding treatment for JA measurements was conducted on fully expanded rosette leaves of 4~5-week-old plants just before bolting by wounding twice across the midrib with a hemostat (42). At indicated times after wounding (Fig. 2), damaged leaves were harvested, weighed, flash frozen in liquid

nitrogen, and stored at −80 °C until processed for JA extraction.

Root growth inhibition assays were conducted with seedlings grown vertically on MS agar medium (0.8% sucrose) in square Petri plates supplemented with JA (10 μM) or coronatine (0.1 μM). Seedlings were grown for 8∼10 days under continuous light (100 μE $m^{-2}$ $s^{-1}$) in a growth chamber maintained at 21 °C.

*Histochemical Staining and Microscopy*—Histochemical detection of GUS activity was as described previously (43). Images of flowers were taken with a Leica MZ16 dissecting microscope. Pollen viability was determined with the fluorescein diacetate (FDA)/propidium iodide (PI) double staining procedure (3). Between 250 and 500 pollen grains were assessed in four independent trials for each genotype with an epifluorescence microscope (Zeiss Axiophot) (excitation at 365 nm, emission at 450 nm longpass). Green fluorescence under UV excitation emitted by de-esterified product of FDA indicates live cells whereas nonviable cells incorporate only PI, which fluoresce red orange under UV light.

For subcellular localization studies, ORFs of *CYP94B3* and *CYP94C1* were PCR amplified from WT genomic DNA using primer sets indicated in supplemental Table S1 and ligated into the XbaI and SalI restriction sites of the binary vector pVKH18En6-mRFP. An internal XbaI restriction site within the *CYP94B3* gene was eliminated by using overlapping PCR to introduce a nonsense mutation (primers FBP-3873 and FBP-3874). Similarly, a SalI restriction site within *CYP94C1* was removed using FBP-3877 and FBP-3878 primer set. The two gene constructs were transiently expressed in *N. tabacum* leaves by syringe-infiltrating the culture suspension of *Agrobacterium* strains harboring each construct. A second strain of *Agrobacterium* contained a construct encoding a soluble ER marker, GFP-HDEL (44), and was co-infiltrated to test co-localization. GFP and mRFP fluorescence was analyzed with an inverted Zeiss LSM 510 Meta Confocal Microscope using microscope settings described earlier (45).

*Heterologous Expression in Yeast and In Vitro Assays*—The *CYP94B1* ORF was PCR amplified from WT *Arabidopsis* genomic DNA template using primers JH3_XmaI_F and JH3_XmaI_R (supplemental Table S1). Subsequent ligation into the XmaI site of yeast expression vector pYeDP60 was followed by transformation into *Saccharomyces cerevisiae* WAT11 strain (46). Preparation of microsomes and *in vitro* hydroxylation assays were described previously (38). Reactions were terminated by adding methanol (to 50% final concentration) containing internal standards for LC-MS/MS analysis.

*In Vitro COI1-JAZ Pull-down Assays*—Constructs and expression of JAZ proteins in *E. coli* were as previously described (25, 27). *In vitro* COI1-JAZ pull-down assays were performed as previously described (25). Ligands used in the COI1-JAZ pull-down assays were enantiomeric mixtures of chemically synthesized JA-Ile and 12COOH-JA-Ile (37).

*Jasmonate Metabolite Analysis*—Jasmonate extraction and analysis by LC-MS/MS was according to previously established methods (47). Transitions from deprotonated molecules to characteristic product ions were monitored in electrospray negative mode for JA-Ile (322→130), [$^{13}C_6$]JA-Ile (328→136), 12OH-JA-Ile (338→130), and 12COOH-JA-Ile (352→130). [$^{13}C_6$]JA-Ile was used as an internal standard for the quantification of JA-Ile and its derivatives. Peak area was integrated using Masslynx software (Waters), and the analytes were quantified based on standard curves generated by comparing analyte responses to the corresponding internal standard. Peak area normalized by the internal standard [$^{13}C_6$]JA-Ile and tissue weight was used to determine the relative abundance of 12COOH-JA-Ile. The 12OH-JA-Ile was a gift from Paul Staswick (University of Nebraska, Lincoln, NE) and [$^{13}C_6$]-JA-Ile was synthesized by conjugation of (±)-JA (Sigma) to [$^{13}C_6$]-L-Ile (Cambridge Isotope Laboratories) (48).

*RNA Analysis*—Total RNA from leaf tissue was extracted using TRIzol reagent (Invitrogen) according to the manufacturer's instructions. RNA blot analysis was as described previously (41). Gene-specific probes for *CYP94B1*, *CYP94B3*, and *Actin-8* (*ACT8*) (At1g49240) were prepared by PCR amplification from genomic DNA template using primers shown in supplemental Table S1. Reverse transcription-PCR was used to detect *CYP94B1* and *CYP94B3* transcripts in *cyp94b1-2cyp94b3-1* double mutant using primers indicated in supplemental Table S1.

## RESULTS

*CYP94B1 Encodes a JA-Ile 12-Hydroxylase*—Previous analyses of wound responses in *cyp94b3* single and *cyp94b3cyp94c1* double mutants suggested that additional enzymes are involved in oxidation of JA-Ile to 12OH-JA-Ile (38–40). Candidates for this activity include uncharacterized members of the CYP94 family, which in *Arabidopsis* consists of six enzymes (20). The deduced amino acid sequence of CYP94B3 is most similar (77% identity) to that of CYP94B1, with both enzymes predicted to have the hallmark features of cytochromes P450 (49). Consistent with the hypothesis that CYP94B1 is a JA-Ile 12-hydroxylase, the wound-inducible expression pattern of the gene (At5g63450) encoding CYP94B1 was similar to that of the CYP94B3-encoding gene (At3g48520) (38, 40). To directly test this hypothesis, we expressed recombinant CYP94B1 in yeast (*S. cerevisiae*) and assayed the capacity of microsomal fractions to produce 12OH-JA-Ile from JA-Ile *in vitro*. Microsomes prepared from yeast cells expressing CYP94B1 produced a compound whose retention time and mass spectrum was identical to an authentic 12OH-JA-Ile standard (Fig. 1*B*, *left panel*). Low but detectable levels of a compound corresponding to 12COOH-JA-Ile ($m/z$ 352 > 130) were also observed in the same reaction mixture (Fig. 1*B*, *right panel*). Control assays performed with microsomes isolated from cells expressing the pYeDP60 empty vector lacked JA-Ile hydroxylase activity (Fig. 1*B*). These results demonstrate that CYP94B1 converts JA-Ile to 12OH-JA-Ile and, to a lesser extent, 12COOH-JA-Ile *in vitro*.

To investigate the biochemical function of CYP94B1 *in planta*, we used LC-MS/MS to measure the wound-induced production of JA-Ile and its oxidized derivatives in a T-DNA insertion mutant (*cyp94b1-1*) that fails to express *CYP94B1* transcripts (data not shown). Consistent with our previous observation (38), the wound-induced accumulation of JA-Ile and 12OH-JA-Ile in wild-type (WT) and *cyp94b1-1* plants was not significantly different (Fig. 2, *A* and *B*). To determine

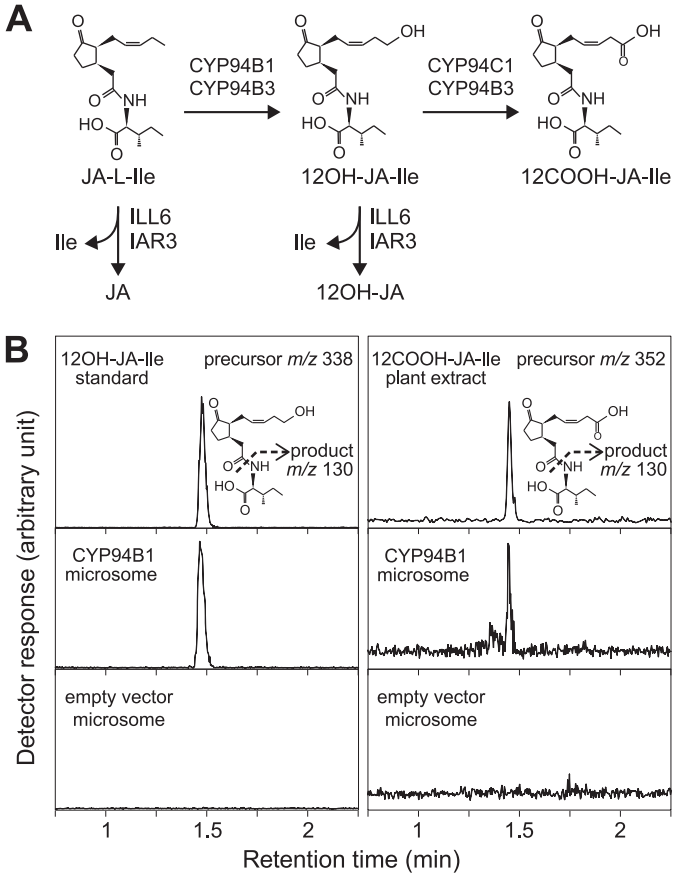


FIGURE 1. **CYP94B1 expressed in yeast catalyzes ω-oxidation of JA-Ile.** *A*, schematic summary of reactions catalyzed by CYP94s and JA amidohydrolases, ILL6 and IAR3. Assignment of enzymes for each step is based on *in vitro* and *in vivo* data described in the text and literatures. *B*, LC chromatogram of products obtained in an *in vitro* JA-Ile hydroxylation assay. Microsomal preparations from yeast transformed with either CYP94B1 or empty vector control were incubated with 50 μM JA-Ile for 2 h. Reaction products were analyzed by LC-MS/MS to detect 12OH-JA-Ile and 12COOH-JA-Ile. Precursor and product ions used for MS/MS detection are shown next to the chromatograms.

whether 12-hydroxylation activity of CYP94B3 compensates for the loss of CYP94B1, we also analyzed a double mutant that lacks both *cyp94b1-1* and *cyp94b3-1*. Wounded leaves of a *cyp94b3-1* single mutant exhibited a significant reduction in 12OH-JA-Ile levels (15% of WT) and also hyper-accumulated JA-Ile (Fig. 2, *A* and *B*), similar to previous reports (38–40). In the *cyp94b1-1cyp94b3-1* double mutant, however, the level of 12OH-JA-Ile was further reduced to ~3% of WT levels (Fig. 2*B*). We also observed that JA-Ile levels in wounded leaves of the double mutant were consistently higher than that in the *cyp94b3-1* single mutant, although this increase was not statistically significant. These hormone profiles were reproduced in a *cyp94b1-2cyp94b3-1* double mutant constructed with an independent mutant allele of *cyp94b1*, *cyp94b1*-2 (data not shown).

We also assessed the *in vivo* enzymatic function of CYP94B1 in transgenic lines (*CYP94B1-OE*) that overexpress *CYP94B1* from the constitutive *Cauliflower Mosaic Virus* (*CaMV*) $^{35}$S promoter. Of 20 independent lines (T1 generation) tested, five showed high constitutive accumulation of *CYP94B1* transcripts and strongly reduced levels of JA-Ile in wounded leaves (data not shown). Side-by-side comparison of selected *CYP94B1-OE* lines with previously characterized *CYP94B3-OE* lines showed that both CYP94Bs have similar effect on wound-induced accumulation of JA-Ile and 12OH-JA-Ile. For example, the level of JA-Ile was only 10 to 20% of that in WT plants at 0.5 and 3 h post wounding (Fig. 2, *C* and *D*). Likewise, wounded leaves of *CYP94B1-OE* and *CYP94B3-OE* plants hyperaccumulated 12OH-JA-Ile (relative to WT) at the 0.5 h time point. The levels of 12OH-JA-Ile in both lines were comparable to that in the WT leaves at the 3 h time point (Fig. 2*D*), which may reflect depletion of JA-Ile substrate (38). These collective findings show that CYP94B1 has JA-Ile 12-hydroxylase activity *in vivo*.

Given that recombinant CYP94B1 converts JA-Ile to 12COOH-JA-Ile *in vitro*, we measured 12COOH-JA-Ile levels in wounded leaves of the mutant (*cyp94b1cyp94b3*) and the overexpressing (*CYP94B1-OE* and *CYP94B3-OE*) lines (Fig. 2, *E* and *F*). The 12COOH-JA-Ile content in wounded leaves of the *cyp94b1cyp94b3* line was only marginally affected, accumulating to ~70% of that in WT leaves 2 h and 3 h after wounding. This finding reflects the major role of CYP94C1 in formation of 12COOH-JA-Ile (40). However, overexpression of CYP94B3 resulted in 1.5 ~ 2.5-fold increase in 12COOH-JA-Ile compared with the WT, indicating the catalytic capacity of CYP94B3 to further oxidize 12OH-JA-Ile to 12COOH-JA-Ile (Fig. 2*F*). Even though recombinant CYP94B1 converted JA-Ile to 12COOH-JA-Ile *in vitro* (Fig. 1*B*), increased 12COOH-JA-Ile level was not observed in the *CYP94B1-OE* plants (Fig. 2*F*).

*The ω-Oxidation and the Hydrolytic Pathways Cooperatively Contribute to JA Homeostasis in Vivo*—In addition to CYP94s, amidohydrolases previously studied for their function in auxin metabolism have been shown to metabolize JA substrates (Fig. 1*A*) (32–34). To test how these two classes of enzymes contribute to JA metabolism, JA profiles in the single and double T-DNA insertion mutants of *cyp94b3-1* and *ill6-1* were compared (Fig. 3). JA-Ile levels were increased in wounded leaves of the *cyp94b3* but not the *ill6-1* single mutant (Fig. 3*B*). Notably, however, JA-Ile levels in the *cyp94b3ill6-1* double mutant were significantly greater than that in the *cyp94b3* single mutant, indicating that both enzymes contribute to JA-Ile catabolism. We also found that the *cyp94b3* and *ill6-1* single mutations decreased and increased, respectively, wound-induced formation of 12OH-JA-Ile, consistent with previous reports (34, 38). Combining the two mutations appeared to cancel these effects, such that the level of 12OH-JA-Ile in the double mutant was comparable to that in WT plants (Fig. 3*D*). Similar to previous observations (34, 38, 40), the wound-induced JA content was not affected by either mutation (Fig. 3*A*). 12OH-JA levels, however, were reduced by the *ill6-1* mutation, indicating that hydrolysis of 12OH-JA-Ile leads to 12OH-JA formation. 12COOH-JA-Ile levels were also significantly increased in wounded leaves of *ill6-1* plants (Fig. 3*E*), presumably due to increased production of its precursor, 12OH-JA-Ile.

*Overexpression of CYP94B1 Results in JA-deficient Phenotypes*—We next studied the physiological effects of CYP94B1 overexpression in *CYP94B1-OE* lines in two well-established JA-mediated physiological processes, fertility and JA-induced root growth inhibition. Five independent T1 lines expressing high levels of *CYP94B1* transcripts displayed defects in fertility (Fig. 4, *panels A–C*). Unlike WT flowers, the stigma of *CYP94B1-OE* flowers protruded through closed petals at devel-

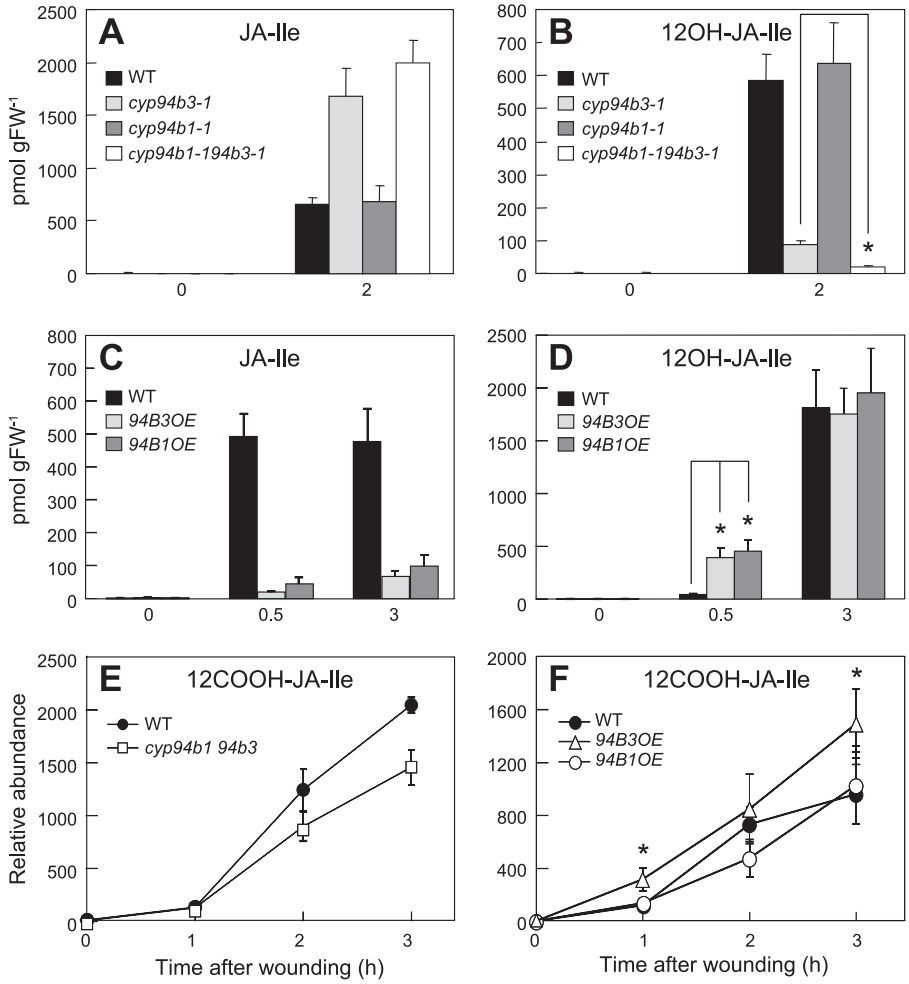


FIGURE 2. **Jasmonate profile in wounded rosette leaves of *CYP94* T-DNA insertion mutants and overexpressing lines.** Rosette leaves were wounded twice across the midrib with a hemostat. Damaged leaves were harvested for JA extraction at indicated times after wounding and analyzed by LC-MS/MS. *A* and *B*, JA-Ile and 12OH-JA-Ile levels in wounded (2 h) and unwounded (0 h) leaves of WT, *cyp94b3-1*, *cyp94b1-1*, and *cyp94b1-1cyp94b3-1* plants. *, $p < 0.001$; Student's *t* test. *C* and *D*, time course of JA-Ile and 12OH-JA-Ile accumulation in wounded leaves of plants overexpressing *CYP94B3* (*94B3OE*) or *CYP94B1* (*94B1OE*). *, $p < 0.01$; Student's *t* test. *E* and *F*, relative abundance of 12COOH-JA-Ile in wounded leaves of WT, *cyp94b1-1cyp94b3-1*, *94B3OE*, and *94B1OE* at various times after wounding. *, $p < 0.05$ between WT and *94B3OE*; Student's *t* test. Each data point represents the mean ± S.D. of three biological replicates.

opmental stages prior to pollination (Fig. 4*B*, *bottom panel*). Elongated stigma papillae were also visible in the infertile flowers (Fig. 4*C*, *right panel*). Anther dehiscence and release of pollen grains occurred without noticeable defects but shorter anther filaments relative to the taller pistils on *CYP94B1-OE* flowers prevented successful pollination (Fig. 4*C*). Pollen collected from *CYP94B1-OE* flowers was also less viable than WT pollen (40~60% WT; Fig. 4*D*).

In addition to reproductive phenotypes, roots of *CYP94B1-OE* seedlings were highly resistant to the growth inhibitory effects of exogenous JA (Fig. 4, *E* and *F*). The extent of insensitivity to JA was not as strong in *CYP94B1-OE* as in *coi1-1*, which have completely lost responsiveness to JA (Fig. 4*F*). To examine if the reduced sensitivity to JA-induced growth inhibitory effects is due to a defect in JA perception or downstream signaling events, root growth inhibition assays were performed with the bacterial toxin coronatine, which is a structural mimic of JA-Ile and potent agonist of the COI1-JAZ receptor (16, 50). Unlike control *coi1-1* seedlings that are insensitive to coronatine, growth of *CYP94B1-OE* roots was as sensitive to coronatine as WT roots, indicating that *CYP94B1-OE* seedlings possess an intact COI1-JAZ signaling system (Fig. 4*G*). This also suggests that coronatine is not a substrate for CYP94B1. Together, these findings demonstrate that overexpression of CYP94B1 depletes JA-Ile to attenuate JA signaling *in vivo*.

*Tissue-specific Expression of CYP94B1 and CYP94B3*—Given the finding that CYP94B1 and CYP94B3 serve a similar biochemical role in oxidation and inactivation of JA-Ile, we next addressed the question of whether the corresponding genes have similar tissue specific expression patterns. The promoter regions of *CYP94B1* (1.8 kb) and *CYP94B3* (2.0 kb) were fused to the β-glucuronidase (GUS)-encoding *uidA* reporter gene and the resulting constructs, designated as *B1pro:GUS* and *B3pro:GUS*, were transformed into *Arabidopsis*. At least 25 independent T1 lines were subject to histochemical staining with 5-bromo-4-chloro-3-indolyl β-glucuronic acid (X-gluc) to determine the range of expression patterns; subsequent experiments were performed with lines exhibiting a representative staining pattern (Fig. 5). Mature rosette leaves of *B1pro:GUS* and *B3pro:GUS* lines displayed a very low background of GUS staining prior to elicitation (Fig. 5, *A* and *B* labeled *UW*). Mechanical wounding and MeJA treatment, however, induced

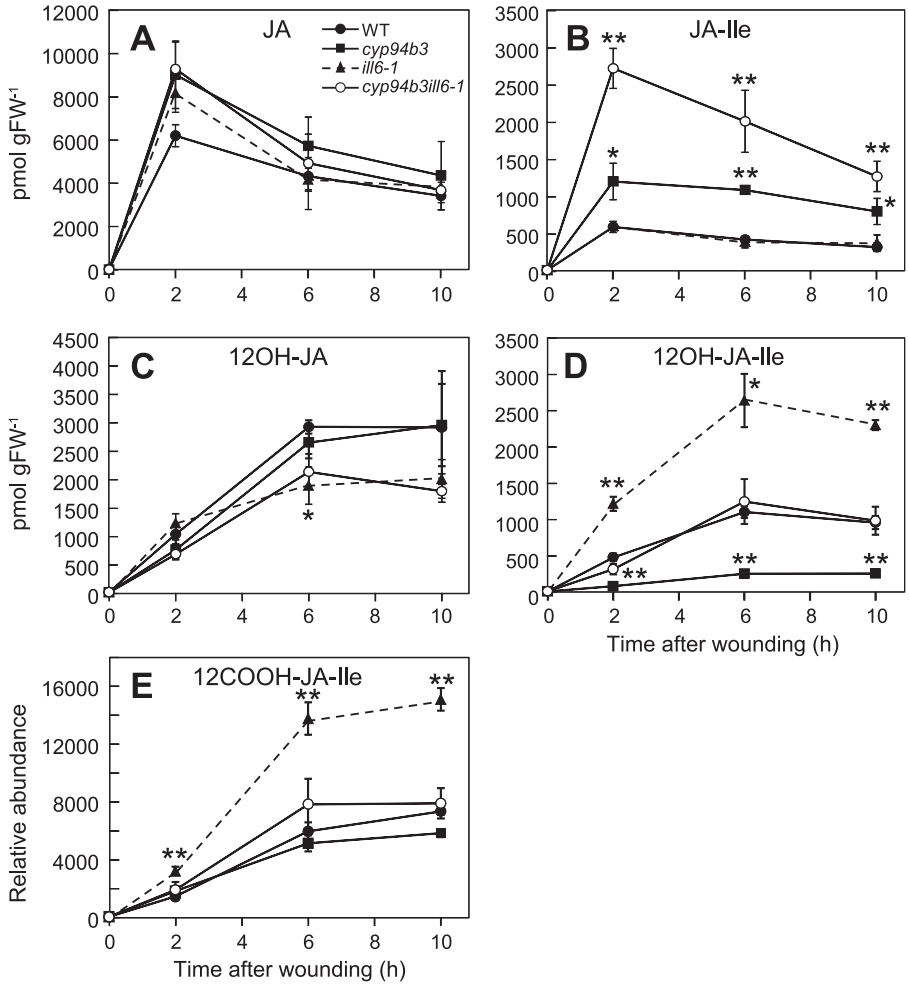


FIGURE 3. **Interaction between two major JA-Ile turnover pathways mediated by CYP94B3 and ILL6.** *A–E*, time course of jasmonate accumulation in wounded rosette leaves of WT, *cyp94b3-1*, *ill6-1*, and *cyp94b3-1ill6-1* plants. *Asterisks* denote significant difference between WT and mutant at $p < 0.01$ (*) or $p < 0.001$ (**); Student's *t* test. Each data point represents the mean ± S.D. of three biological replicates.

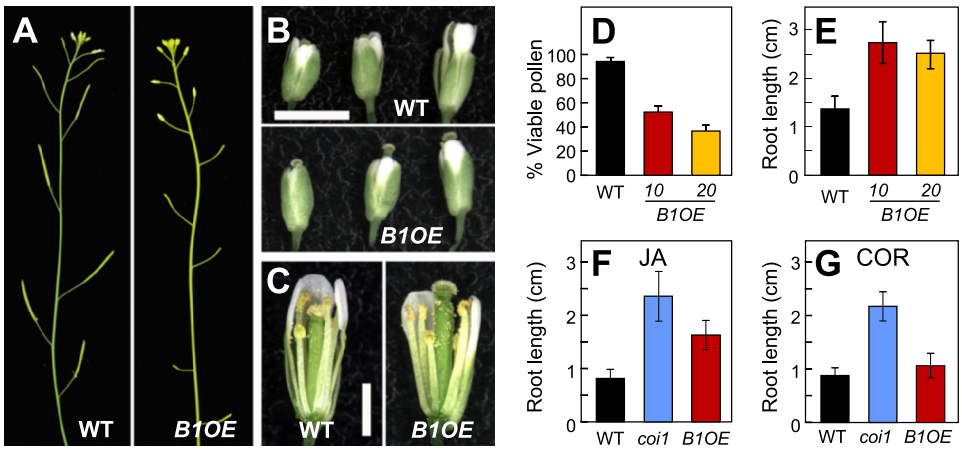


FIGURE 4. **CYP94B1-OE plants display JA-resistant phenotypes in roots and flowers.** *A*, photographs showing silique development in WT (*left panel*) and *CYP94B1-OE* (*right*). *B*, photographs of representative WT (*top panel*) and *CYP94B1-OE* (*bottom*) flowers at three developmental stages. Scale bar, 2 mm. *C*, developing stamens and pistils of WT (*left*) and *CYP94B1-OE* (*right*) at time of pollination. Petals and sepals were removed to expose the interior parts of flowers. Scale bar, 1 mm. *D*, pollen viability of WT and two independent homozygous lines of *CYP94B1-OE* (*B1OE-10* and *B1OE-20*). Pollen viability was assessed in four independent trials. *E - G*, root growth inhibition assays. WT, *CYP94B1-OE* (*B1OE*), and *coi1-1* were grown on MS medium containing either 10 μM jasmonic acid (*E*, *F*) or 0.1 μM coronatine (COR) (*G*). Root length was determined on 10-d (*E*, *F*) or 8-d (*G*) old plants. Data show the mean ± S.D. ($n > 20$).

GUS expression patterns that were spatially distinct between the two lines (Fig. 5, *A–C*). Wounding activated *B1pro:GUS* expression mainly in the vascular regions, whereas it elicited very strong expression of the *B3pro:GUS* reporter throughout the leaf lamina (Fig. 5*B*). MeJA treatment induced GUS expression in both reporter lines, with staining in *B3pro:*

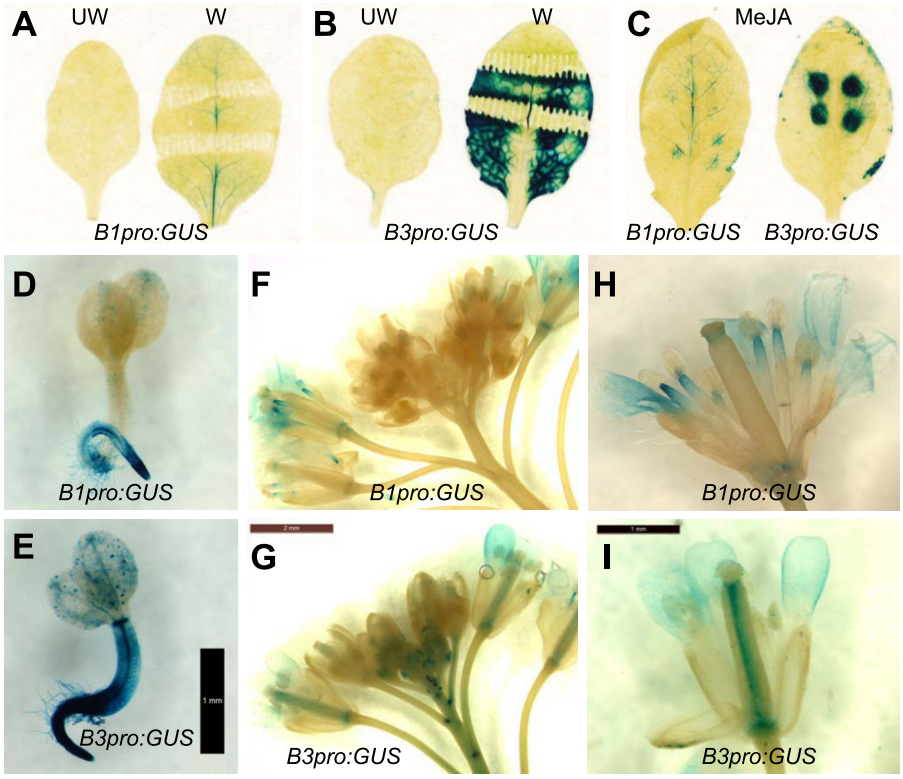


FIGURE 5. **Tissue-specific expression of *CYP94B1* and *CYP94B3*.** *A* and *B*, X-gluc staining of control unwounded (*UW*) or wounded (*W*) (for 24 h) leaves of *CYP94B1promoter:GUS* (*B1pro:GUS*) and *CYP94B3promoter:GUS* (*B3pro:GUS*) plants. *C*, *B1pro:GUS* (*left panel*) and *B3pro:GUS* (*right*) leaves treated with MeJA (for 24 h). Several droplets (10 $\mu$l) of a solution containing 50 $\mu$M MeJA were spotted onto the leaf surface. *D* and *E*, X-gluc staining of *B1pro:GUS* and *B3pror:GUS* seedlings 2∼3-days after germination. Bar, 1 mm. *F-I*, influorescence and flowers of *B1pro:GUS* and *B3pro:GUS*. Bars, 2 mm (*G*) and 1 mm (*I*).

*GUS* being more intense (Fig. 5*C*). GUS staining in the *B3pro:GUS* was more spatially restricted to the site of MeJA application, producing dark blue circles with sharply defined borders (Fig. 5*C*, *right panel*). More prominent staining in the vascular system was observed in MeJA-treated *B3pro:GUS* leaves (Fig. 5*C*).

GUS staining of whole seedlings and reproductive tissue also revealed differences in the spatial expression pattern of *CYP94B1* and *CYP94B3*. In seedlings, expression of *B1pro:GUS* was largely restricted to the roots (Fig. 5*D*), whereas *B3pro:GUS* was highly expressed both in the shoot and root (Fig. 5*E*). In the influorescence, *B3pro:GUS* was expressed in younger unopened buds as well as in opened mature flowers (Fig. 5, *G* and *I*), whereas *B1pro:GUS* was expressed predominantly in opened mature flowers (Fig. 5, *F* and *H*). Within the flower, *CYP94B1* was expressed in the stamen at the joint between anther and filament. *CYP94B3* expression was more localized to the center of pistil. Additionally, *CYP94B3* was expressed strongly at the base of the initiating lateral peduncles. Both genes were expressed in petals (Fig. 5, *F-I*) but neither gene appeared to be expressed in mature pollen, where some JA biosynthetic genes are expressed (3, 43). In summary, results from these promoter-GUS studies show that *CYP94B1* and *CYP94B3* have both overlapping and distinct tissue-specific expression patterns.

*Subcellular Localization of JA-Ile-oxidizing CYP94 Enzymes*—The cytosolic location of JA-Ile-conjugation (51), together with the site of JA-Ile perception in the nucleus (52), raises the question about the site of JA-Ile inactivation. Although many P450s reside in the ER facing the cytosolic side (49, 53), there are examples of plant P450s that are localized to other subcellular compartments, including mitochondria (54, 55) and chloroplasts (56, 57). We therefore determined the subcellular location of CYP94B3 and CYP94C1 by generating constructs in which the monomeric red fluorescent protein (mRFP) was fused to the C terminus of CYP94B3 and CYP94C1, designated *CYP94B3-mRFP* and *CYP94C1-mRFP*, respectively. An *Agrobacterium tumefaciens* co-infiltration assay (44) was used to transiently co-express these constructs in tobacco (*N. tabacum*) leaves along with a soluble ER localization marker fused to the green fluorescent protein (GFP-HDEL) (44). Laser scanning confocal microscopy analyses of the *CYP94B3-mRFP* and *CYP94C1-mRFP* infiltrated leaves produced images typical of the ER network. The ER localization pattern was confirmed by the overlap of the ER marker GFP-HDEL with that of CYP94B3-mRFP and CYP94C1-mRFP (Fig. 6). These findings indicate that the ER is the site of JA-Ile oxidative turnover by CYP94 P450s.

*12COOH-JA-Ile Is Inactive in Promoting COI1-JAZ Interaction*—It was previously observed that although 12OH-JA-Ile is less effective than JA-Ile in promoting COI1-JAZ interaction, this oxidized derivative maintains some activity as a receptor ligand (38). To test whether further oxidation to 12COOH-JA-Ile has a more pronounced effect on receptor activation, we used an *in vitro* pull-down assay (Fig. 7*A*) (14, 16, 27) to compare the ability of JA-Ile and 12COOH-JA-Ile to promote the COI1 interaction with four representative JAZ substrates. As shown in Fig. 7, JA-Ile stimulated COI1 binding to JAZ2, JAZ10,

and JAZ12 in a dose-dependent manner, as previously reported (25, 27). 12COOH-JA-Ile, however, was largely inactive in promoting COI1-JAZ interaction with all JAZs tested (Fig. 7). We also found that 12COOH-JA-Ile fails to promote interaction of COI1 with JAZ8 (Fig. 7*E*), which contains a non-canonical degron that binds COI1 in the presence of coronatine but not JA-Ile (27).

## DISCUSSION

Hydroxylation is commonly used in detoxification pathways to convert hydrophobic toxic chemicals into more water-soluble products to be stored away from active sites or to be excreted (58, 59). Overactivation of JA pathway can have "toxic" effects on plants, for instance, by causing growth arrest. Multiple lines of evidence presented in this paper demonstrate that CYP94B1 is a JA-Ile-12-hydroxylase that participates in metabolic inactivation of the JA-Ile signal.

Recombinant CYP94B1 expressed in yeast converted JA-Ile substrate into 12OH-JA-Ile and also to lesser amounts of 12COOH-JA-Ile. Two consecutive oxidations of JA-Ile to 12COOH-JA-Ile were previously observed with CYP94B3 and CYP94C1, with major products being 12OH-JA-Ile and 12COOH-JA-Ile, respectively (38, 40). Our results indicate that CYP94B1, like B3, acts primarily in catalysis of the first hydroxylation step. That wound-induced formation of 12OH-JA-Ile in the leaves of the *cyp94b1cyp94b3* double mutant was reduced to only 3% of that in WT indicates that CYP94B1 and CYP94B3 account for ~ 97% of the 12-hydroxylation activity *in vivo*. The remainder may result from combined contributions by other CYP94 subfamily enzymes such as CYP94B2 or CYP94C1. Considering the near complete depletion of 12OH-JA-Ile in wounded *cyp94b1cyp94b3* leaves (Fig. 2*B*), it was unexpected that the production of 12COOH-JA-Ile in this mutant was maintained at near (70%) WT levels (Fig. 2*E*). This implies that CYP94C1 can catalyze two consecutive oxidation steps using JA-Ile as substrate. On the other hand, the fact that loss of CYP94C1, which is the major enzyme for 12COOH-JA-Ile formation, results in only a ~50% reduction in 12COOH-JA-Ile, implies the existence of another enzyme(s) that can catalyze 12COOH-JA-Ile formation. A near-to-complete loss of 12COOH-JA-Ile in *cyp94b3cyp94c1* (40) indicates that CYP94B3 is directly involved in 12COOH-JA-Ile formation *in vivo*, especially in the absence of CYP94C1. Increased accumulation of 12COOH-JA-Ile in *CYP94B3-OE* (Fig. 2*F*) also supports a role for CYP94B3 in the formation of 12COOH-JA-Ile. Overexpression of CYP94B1 did not increase the level of 12COOH-JA-Ile over WT, despite its ability to phenocopy the

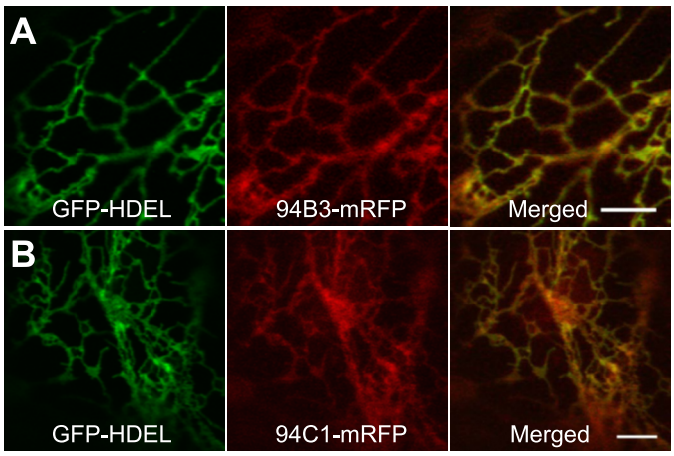


FIGURE 6. **Subcellular localization of CYP94B3 and CYP94C1.** Confocal images of tobacco leaf epidermal cells co-expressing the GFP-HDEL ER marker (*left panel* of *A* and *B*), and either CYP94B3 (94B3-mRFP) or CYP94C1 (94C1-mRFP) fused to the monomeric red fluorescent protein (*middle panel* of *A* and *B*). Merge between GFP and mRFP indicates co-localization (*right panel* of *A* and *B*). Bars, 5 $\mu$m.

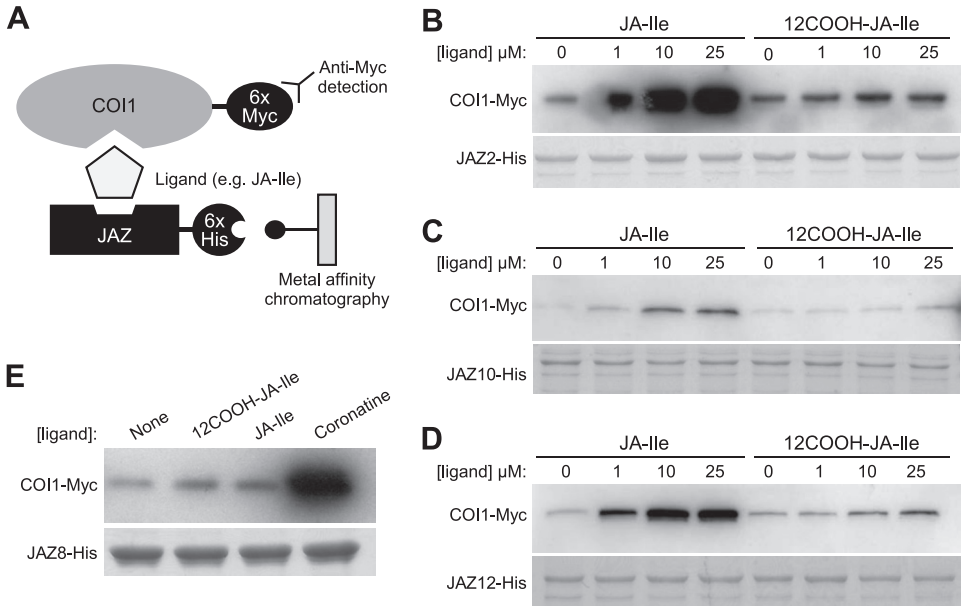


FIGURE 7. **12COOH-JA-Ile does not promote assembly of COI1-JAZ receptor complexes.** *A*, schematic of *in vitro* pull-down assays. Ligand-dependent interaction between COI1 and (*B*) JAZ2, (*C*) JAZ10, (*D*) JAZ12, and (*E*) JAZ8. Pull-down assays were performed using recombinant JAZ-His protein and crude leaf extract from *Arabidopsis* plants expressing $^{35}$*S:COI1-Myc* in the presence of the indicated concentrations of JA-Ile, 12COOH-JA-Ile or coronatine. Reactions with JAZ8 contained 25 $\mu$M of 12COOH-JA-Ile and JA-Ile or 2.5 $\mu$M coronatine. Equal recovery and loading of JAZ-His protein is indicated by a Coomassie Blue-stained acrylamide gel.

effects of *CYP94B3-OE* on JA-Ile and 12OH-JA-Ile levels (Fig. 2, *D* and *F*). Therefore, our collective results indicate that CYP94B1 is mainly involved in the initial oxidation of JA-Ile to 12OH-JA-Ile, but that a role for this CYP94 member in metabolism of other substrates cannot be excluded.

The decline in 12OH-JA-Ile levels in the *cyp94b3cyp94c1* double mutant, in which 12OH-JA-Ile conversion to 12COOH-JA-Ile is blocked (40), indicates pathways for 12OH-JA-Ile metabolism other than oxidization to 12COOH-JA-Ile. A recently reported *O*-linked glucosyl derivative of 12OH-JA-Ile (37) could potentially serve as a sink for 12OH-JA-Ile. Additionally, 12OH-JA-Ile is hydrolyzed to 12OH-JA and Ile by the IAR3 and ILL6 members of the amidohydrolase superfamily in *Arabidopsis* (33, 34) and homologous enzymes (JIH1) in tobacco (32). Even though the effect of ILL6 mutation on JA-Ile level was minimal in the *ill6-1* single mutant (Fig. 3*B*) (34), additional loss of CYP94B3 function created a major blockage in JA-Ile turnover and, consequently, a massive accumulation of JA-Ile in the *cyp94b3ill6-1* double mutant. Together with the reported *in vitro* hydrolytic activity (33, 34), this genetic evidence confirms the function of ILL6 in JA-Ile turnover *in vivo*. It remains to be determined whether the '$\omega$-oxidation' and the hydrolysis pathways catalyzed by CYP94s and amidohydrolases, respectively, are solely responsible for JA-Ile catabolism, or whether additional pathways are involved (*e.g.* methylation). Higher order knock-out mutants defective in multiple CYP94s and amidohydrolases will help answer this question.

Strong JA-deficient phenotypes created by overexpressing CYP94B1 indicates that increased flux through $\omega$-oxidation leads to deactivation of JA signaling, implying that the oxidized products are inactive in inducing JA responses. Our previous study showed that 12OH-JA-Ile is significantly reduced in its ability to promote interaction between COI1 and JAZs but retains some activity (38). Therefore, we could not exclude the possibility that 12OH-JA-Ile associates with the receptor *in vivo*. We show here that 12COOH-JA-Ile is essentially inactive in promoting COI1 interaction with a broad range of JAZ substrates, indicating that consecutive oxidation of JA-Ile to 12COOH-JA-Ile is an effective means to terminate signaling (Fig. 7). Additional modifications to the C12 hydroxy group, such as sulfation or glucosylation, may also inhibit COI1-JAZ complex-promoting activity by restricting entry of the ligand into the binding pocket of COI1 (50). Additional structural studies are needed to better understand how modification of JA-Ile by CYP94 P450s and other enzymes affect ligand interaction with the COI1-JAZ co-receptor system.

In addition to the compromised receptor binding capacity, altered physical properties (*e.g.* polarity) may play role in the loss of signaling activity by oxidized JA-Ile derivatives, for example by changing their subcellular partitioning. The subcellular distribution of various JA derivatives is not well understood. Our subcellular localization of CYP94B3 and CYP94C1 demonstrates the ER as the major site for JA-Ile oxidation. Given the established topology of many P450s in ER membranes (49, 53), we presume that the CYP94 N terminus is imbedded in the ER with the enzyme's active site facing the cytosol. Even though CYP94B1 was not tested for its subcellular location, the similarities of this isoform with CYP94B3 suggest that it also localizes to the ER. It is plausible that JA metabolites are rapidly exchanged between the nucleus and the ER through lateral diffusion in the ER membrane, which forms a continuum with the outer membrane of the nuclear envelope (60). The molecular organization of JA-metabolizing enzymes and metabolites in multiple subcellular compartments needs further investigation. Given the known biological activities of some oxidized- and glucosylated JAs (61, 62), it is also possible that these JA-Ile derivatives may have molecular targets other than the COI1.

The promoter-GUS reporters of CYP94B1 and CYP94B3 revealed their tissue specific expression patterns. Notable differences in the expression pattern of these two genes include: i) in reproductive organs where *CYP94B1* was strongly expressed (*e.g.* upper anther filament), *CYP94B3* expression was not detected; ii) in wounded leaves where *CYP94B1* expression was strongest (*e.g.* in vascular tissues), expression of *CYP94B3* was more evenly dispersed in all cell types; and iii) in seedlings where *CYP94B1* expression was largely restricted to the roots. In the inflorescence stems, *CYP94B3* was also strongly expressed at the base of the initiating lateral peduncles, reminiscent of the expression of *lateral organ boundaries* (*LOB*) gene, recently shown to function in defining organ boundaries through interplay with brassinosteroids (63).

The combined effects of the hydrolysis pathway catalyzed by amidohydrolases and the $\omega$-oxidation pathway catalyzed by CYP94s represent an evolutionarily conserved mechanism to maintain optimal levels of the potent JA-Ile signal. At least 70 CYP94-like sequences have been reported in sequenced plant genomes (20). The vast majority of these have not been characterized (59, 64) but based on function of *Arabidopsis* CYP94s, many of them are expected to be involved in metabolism of JAs. Likewise, although auxin amidohydrolases have been characterized in only a handful of plant species (65, 66), their related sequences have been reported from many plant species (67). In addition to their conservation across higher plants, tight co-regulation of these pathways (33, 34, 38, 40) implies selection pressure to limit the production of JA-Ile and thereby attenuate the strength of JA responses. Reverse genetic approaches aimed at blocking all catabolic steps may be useful to elucidate those essential functions of JA-Ile catabolism. Attenuation of the JA signal depends also on other mechanisms, including negative transcriptional control of JA responses that are also tightly co-regulated with JA-regulated genes (24, 25, 27, 28). Additional studies are needed to understand how the concerted action of these various negative feedback loops restrains JA-responses and impacts plant growth under various stress conditions.

*Acknowledgments—We thank Nizam Zubir Mohamad, Noor Kamila Ahmad Shafiai, Li Zhang, Thomas Marcink, Priya Bariya, and Hannah Wahl for technical assistance. We are grateful to Paul Staswick for providing 12OH-JA-Ile, Joe Chappell for providing yeast strain WAT11, John Browse for ill6-1 seeds, Sheng Yang He for providing the Arabidopsis $^{35}$S:COI1-Myc line, and the Arabidopsis Biological Resource Center for providing T-DNA insertion lines.*

## REFERENCES


1. Glazebrook, J. (2005) Contrasting mechanisms of defense against biotrophic and necrotrophic pathogens. *Annu. Rev. Phytopathol.* **43,** 205–227
2. Wasternack, C., and Hause, B. (2013) Jasmonates: biosynthesis, perception, signal transduction and action in plant stress response, growth and development. *Ann. Bot.* **111,** 1021–1058
3. McConn, M., and Browse, J. (1996) The critical requirement for linolenic acid is pollen development, not photosynthesis, in an *Arabidopsis* mutant. *Plant Cell* **8,** 403–416
4. Li, L., Zhao, Y., McCaig, B. C., Wingerd, B. A., Wang, J., Whalon, M. E., Pichersky, E., and Howe, G. A. (2004) The tomato homolog of CORONATINE-INSENSITIVE1 is required for the maternal control of seed maturation, jasmonate-signaled defense responses, and glandular trichome development. *Plant Cell* **16,** 126–143
5. Zhang, Y., and Turner, J. (2008) Wound-induced endogenous jasmonates stunt plant growth by inhibiting mitosis. *PLoS ONE* **3,** e3699
6. Song, S., Qi, T., Wasternack, C., and Xie, D. (2014) Jasmonate signaling and crosstalk with gibberellin and ethylene. *Curr. Opin. Plant Biol.* **21,** 112–119
7. Vanstraelen, M., and Benková, E. (2012) Hormonal interactions in the regulation of plant development. *Annu. Rev. Cell Dev. Biol.* **28,** 463–487
8. Browse, J. (2009) Jasmonate passes muster: a receptor and targets for the defense hormone. *Annu. Rev. Plant Biol.* **60,** 183–205
9. Koo, A. J., and Howe, G. A. (2009) The wound hormone jasmonate. *Phytochemistry* **70,** 1571–1580
10. Fonseca, S., Chini, A., Hamberg, M., Adie, B., Porzel, A., Kramell, R., Miersch, O., Wasternack, C., and Solano, R. (2009) (+)-7-iso-Jasmonoyl-L-isoleucine is the endogenous bioactive jasmonate. *Nat. Chem. Biol.* **5,** 344–350
11. Schaller, A., and Stintzi, A. (2009) Enzymes in jasmonate biosynthesis - structure, function, regulation. *Phytochemistry* **70,** 1532–1538
12. Westfall, C. S., Zubieta, C., Herrmann, J., Kapp, U., Nanao, M. H., and Jez, J. M. (2012) Structural basis for prereceptor modulation of plant hormones by GH3 proteins. *Science* **336,** 1708–1711
13. Yan, Y., Stolz, S., Chételat, A., Reymond, P., Pagni, M., Dubugnon, L., and Farmer, E. E. (2007) A downstream mediator in the growth repression limb of the jasmonate pathway. *Plant Cell* **19,** 2470–2483
14. Thines, B., Katsir, L., Melotto, M., Niu, Y., Mandaokar, A., Liu, G., Nomura, K., He, S. Y., Howe, G. A., and Browse, J. (2007) JAZ repressor proteins are targets of the SCF(COI1) complex during jasmonate signalling. *Nature* **448,** 661–665
15. Chini, A., Fonseca, S., Fernández, G., Adie, B., Chico, J. M., Lorenzo, O., García-Casado, G., López-Vidriero, I., Lozano, F. M., Ponce, M. R., Micol, J. L., and Solano, R. (2007) The JAZ family of repressors is the missing link in jasmonate signalling. *Nature* **448,** 666–671
16. Katsir, L., Schilmiller, A. L., Staswick, P. E., He, S. Y., and Howe, G. A. (2008) COI1 is a critical component of a receptor for jasmonate and the bacterial virulence factor coronatine. *Proc. Natl. Acad. Sci. U.S.A.* **105,** 7100–7105
17. Yang, D. L., Yao, J., Mei, C. S., Tong, X. H., Zeng, L. J., Li, Q., Xiao, L. T., Sun, T. P., Li, J., Deng, X. W., Lee, C. M., Thomashow, M. F., Yang, Y., He, Z., and He, S. Y. (2012) Plant hormone jasmonate prioritizes defense over growth by interfering with gibberellin signaling cascade. *Proc. Natl. Acad. Sci. U.S.A.* **109,** E1192–E1200
18. Noir, S., Bömer, M., Takahashi, N., Ishida, T., Tsui, T. L., Balbi, V., Shanahan, H., Sugimoto, K., and Devoto, A. (2013) Jasmonate controls leaf growth by repressing cell proliferation and the onset of endoreduplication while maintaining a potential stand-by mode. *Plant Physiol.* **161,** 1930–1951
19. Ullmann-Zeunert, L., Stanton, M. A., Wielsch, N., Bartram, S., Hummert, C., Svatoš, A., Baldwin, I. T., and Groten, K. (2013) Quantification of growth–defense trade-offs in a common currency: nitrogen required for phenolamide biosynthesis is not derived from ribulose-1,5-bisphosphate carboxylase/oxygenase turnover. *Plant J.* **75,** 417–429
20. Koo, A. J., and Howe, G. A. (2012) Catabolism and deactivation of the lipid-derived hormone jasmonoyl-isoleucine. *Front. Plant Sci.* **3,** 19
21. Huot, B., Yao, J., Montgomery, B. L., and He, S. Y. (2014) Growth-defense tradeoffs in plants: a balancing act to optimize fitness. *Mol. Plant* **7,** 1267–1287
22. Campos, M. L., Kang, J. H., and Howe, G. A. (2014) Jasmonate-triggered plant immunity. *J. Chem. Ecol.* **40,** 657–675
23. Chung, H. S., Koo, A. J., Gao, X., Jayanty, S., Thines, B., Jones, A. D., and Howe, G. A. (2008) Regulation and function of *Arabidopsis* JASMONATE ZIM-domain genes in response to wounding and herbivory. *Plant Physiol.* **146,** 952–964
24. Moreno, J. E., Shyu, C., Campos, M. L., Patel, L. C., Chung, H. S., Yao, J., He, S. Y., and Howe, G. A. (2013) Negative feedback control of jasmonate signaling by an alternative splice variant of JAZ10. *Plant Physiol.* **162,** 1006–1017
25. Chung, H. S., and Howe, G. A. (2009) A critical role for the TIFY motif in repression of jasmonate signaling by a stabilized splice variant of the JASMONATE ZIM-domain protein JAZ10 in *Arabidopsis*. *Plant Cell* **21,** 131–145
26. Chung, H. S., Niu, Y., Browse, J., and Howe, G. A. (2009) Top hits in contemporary JAZ: an update on jasmonate signaling. *Phytochemistry* **70,** 1547–1559
27. Shyu, C., Figueroa, P., Depew, C. L., Cooke, T. F., Sheard, L. B., Moreno, J. E., Katsir, L., Zheng, N., Browse, J., and Howe, G. A. (2012) JAZ8 lacks a canonical degron and has an EAR motif that mediates transcriptional repression of jasmonate responses in *Arabidopsis*. *Plant Cell* **24,** 536–550
28. Nakata, M., Mitsuda, N., Herde, M., Koo, A. J., Moreno, J. E., Suzuki, K., Howe, G. A., and Ohme-Takagi, M. (2013) A bHLH-type transcription factor, ABA-inducible BHLH-type transcription factor/JA-associated MYC2-like1, acts as a repressor to negatively regulate jasmonate signaling in *Arabidopsis*. *Plant Cell* **25,** 1641–1656
29. Sasaki-Sekimoto, Y., Jikumaru, Y., Obayashi, T., Saito, H., Masuda, S., Kamiya, Y., Ohta, H., and Shirasu, K. (2013) Basic helix-loop-helix transcription factors Jasmonate-associated MYC2-like1 (JAM1), JAM2, and JAM3 are negative regulators of jasmonate responses in *Arabidopsis*. *Plant Physiol.* **163,** 291–304
30. Song, S., Qi, T., Fan, M., Zhang, X., Gao, H., Huang, H., Wu, D., Guo, H., and Xie, D. (2013) The bHLH subgroup IIId factors negatively regulate jasmonate-mediated plant defense and development. *PLoS Genet.* **9,** e1003653
31. Fonseca, S., Fernández-Calvo, P., Fernández, G. M., Díez-Díaz, M., Gimenez-Ibanez, S., Lopez-Vidriero, I., Godoy, M., Fernández-Barbero, G., Van Leene, J., De Jaeger, G., Franco-Zorrilla, J. M., and Solano, R. (2014) bHLH003, bHLH013 and bHLH017 are new targets of JAZ repressors negatively regulating JA responses. *PLoS ONE* **9,** e86182
32. Woldemariam, M. G., Onkokesung, N., Baldwin, I. T., and Galis, I. (2012) Jasmonoyl-l-isoleucine hydrolase 1 (JIH1) regulates jasmonoyl-l-isoleucine levels and attenuates plant defenses against herbivores. *Plant J.* **72,** 758–767
33. Bhosale, R., Jewell, J. B., Hollunder, J., Koo, A. J., Vuylsteke, M., Michoel, T., Hilson, P., Goossens, A., Howe, G. A., Browse, J., and Maere, S. (2013) Predicting gene function from uncontrolled expression variation among individual wild-type *Arabidopsis* plants. *Plant Cell* **25,** 2865–2877
34. Widemann, E., Miesch, L., Lugan, R., Holder, E., Heinrich, C., Aubert, Y., Miesch, M., Pinot, F., and Heitz, T. (2013) The amidohydrolases IAR3 and ILL6 contribute to jasmonoyl-isoleucine hormone turnover and generate 12-hydroxyjasmonic acid upon wounding in *Arabidopsis* leaves. *J. Biol. Chem.* **288,** 31701–31714
35. Glauser, G., Grata, E., Dubugnon, L., Rudaz, S., Farmer, E. E., and Wolfender, J. L. (2008) Spatial and temporal dynamics of jasmonate synthesis and accumulation in *Arabidopsis* in response to wounding. *J. Biol. Chem.* **283,** 16400–16407
36. Guranowski, A., Miersch, O., Staswick, P. E., Suza, W., and Wasternack, C. (2007) Substrate specificity and products of side-reactions catalyzed by jasmonate:amino acid synthetase (JAR1). *FEBS Lett.* **581,** 815–820
37. Kitaoka, N., Kawaide, H., Amano, N., Matsubara, T., Nabeta, K., Takahashi, K., and Matsuura, H. (2014) CYP94B3 activity against jasmonic acid amino acid conjugates and the elucidation of 12-O-$\beta$-glucopyranosyl-jasmonoyl-L-isoleucine as an additional metabolite. *Phytochemistry* **99,** 6–13
38. Koo, A. J., Cooke, T. F., and Howe, G. A. (2011) Cytochrome P450

CYP94B3 mediates catabolism and inactivation of the plant hormone jasmonoyl-L-isoleucine. *Proc. Natl. Acad. Sci. U.S.A.* **108,** 9298–9303
39. Kitaoka, N., Matsubara, T., Sato, M., Takahashi, K., Wakuta, S., Kawaide, H., Matsui, H., Nabeta, K., and Matsuura, H. (2011) *Arabidopsis* CYP94B3 encodes jasmonyl-L-isoleucine 12-hydroxylase, a key enzyme in the oxidative catabolism of jasmonate. *Plant Cell Physiol.* **52,** 1757–1765
40. Heitz, T., Widemann, E., Lugan, R., Miesch, L., Ullmann, P., Désaubry, L., Holder, E., Grausem, B., Kandel, S., Miesch, M., Werck-Reichhart, D., and Pinot, F. (2012) Cytochromes P450 CYP94C1 and CYP94B3 catalyze two successive oxidation steps of plant hormone Jasmonoyl-isoleucine for catabolic turnover. *J. Biol. Chem.* **287,** 6296–6306
41. Koo, A. J. K., Chung, H. S., Kobayashi, Y., and Howe, G. A. (2006) Identification of a peroxisomal acyl-activating enzyme involved in the biosynthesis of jasmonic acid in *Arabidopsis*. *J. Biol. Chem.* **281,** 33511–33520
42. Herde, M., Koo, A. K., and Howe, G. (2013) Elicitation of jasmonate-mediated defense responses by mechanical wounding and insect herbivory in *Jasmonate Signaling* (Goossens, A., and Pauwels, L. eds), pp. 51–61, Humana Press
43. Schilmiller, A. L., Koo, A. J., and Howe, G. A. (2007) Functional diversification of acyl-coenzyme A oxidases in jasmonic acid biosynthesis and action. *Plant Physiol.* **143,** 812–824
44. Brandizzi, F., Hanton, S., DaSilva, L. L., Boevink, P., Evans, D., Oparka, K., Denecke, J., and Hawes, C. (2003) ER quality control can lead to retrograde transport from the ER lumen to the cytosol and the nucleoplasm in plants. *Plant J.* **34,** 269–281
45. Brandizzi, F., Fricker, M., and Hawes, C. (2002) A greener world: The revolution in plant bioimaging. *Nat. Rev. Mol. Cell Biol.* **3,** 520–530
46. Pompon, D., Louerat, B., Bronine, A., and Urban, P. (1996) Yeast expression of animal and plant P450s in optimized redox environments. *Methods Enzymol.* **272,** 51–64
47. Koo, A. J., Gao, X., Jones, A. D., and Howe, G. A. (2009) A rapid wound signal activates the systemic synthesis of bioactive jasmonates in *Arabidopsis*. *Plant J.* **59,** 974–986
48. Kramell, R., Schmidt, J., Schneider, G., Sembdner, G., and Schreiber, K. (1988) Synthesis of *N*-(jasmonoyl) amino acid conjugates. *Tetrahedron* **44,** 5791–5807
49. Werck-Reichhart, D. l., Bak, S. r., and Paquette, S. (2009) Cytochromes P450 in *The Arabidopsis Book*, The American Society of Plant Biologists, pp. 1–28
50. Sheard, L. B., Tan, X., Mao, H., Withers, J., Ben-Nissan, G., Hinds, T. R., Kobayashi, Y., Hsu, F. F., Sharon, M., Browse, J., He, S. Y., Rizo, J., Howe, G. A., and Zheng, N. (2010) Jasmonate perception by inositol-phosphate-potentiated COI1-JAZ co-receptor. *Nature* **468,** 400–405
51. Hsieh, H. L., Okamoto, H., Wang, M., Ang, L. H., Matsui, M., Goodman, H., and Deng, X. W. (2000) FIN219, an auxin-regulated gene, defines a link between phytochrome A and the downstream regulator COP1 in light control of *Arabidopsis* development. *Genes Dev.* **14,** 1958–1970
52. Withers, J., Yao, J., Mecey, C., Howe, G. A., Melotto, M., and He, S. Y. (2012) Transcription factor-dependent nuclear localization of a transcriptional repressor in jasmonate hormone signaling. *Proc. Natl. Acad. Sci. U.S.A.* **109,** 20148–20153
53. Yamamoto, K., Gildenberg, M., Ahuja, S., Im, S.-C., Pearcy, P., Waskell, L., and Ramamoorthy, A. (2013) Probing the transmembrane structure and topology of cicrosomal cytochrome-P450 by solid-state NMR on temperature-resistant bicelles. *Sci. Rep.* **3,** 2556
54. Benveniste, I., Salaün, J.-P., and Durst, F. (1978) Phytochrome-mediated regulation of a monooxygenase hydroxylating cinnamic acid in etiolated pea seedlings. *Phytochemistry* **17,** 359–363
55. Okuda, K. I. (1994) Liver mitochondrial P450 involved in cholesterol catabolism and vitamin D activation. *J. Lipid Res.* **35,** 361–372
56. Froehlich, J. E., Itoh, A., and Howe, G. A. (2001) Tomato allene oxide synthase and fatty acid hydroperoxide lyase, two cytochrome P450s involved in oxylipin metabolism, are targeted to different membranes of chloroplast envelope. *Plant Physiol.* **125,** 306–317
57. Helliwell, C. A., Sullivan, J. A., Mould, R. M., Gray, J. C., Peacock, W. J., and Dennis, E. S. (2001) A plastid envelope location of *Arabidopsis* ent-kaurene oxidase links the plastid and endoplasmic reticulum steps of the gibberellin biosynthesis pathway. *Plant J.* **28,** 201–208
58. Hardwick, J. P. (2008) Cytochrome P450 omega hydroxylase (CYP4) function in fatty acid metabolism and metabolic diseases. *Biochem. Pharmacol.* **75,** 2263–2275
59. Pinot, F., and Beisson, F. (2011) Cytochrome P450 metabolizing fatty acids in plants: characterization and physiological roles. *FEBS J.* **278,** 195–205
60. Goldberg, M. W., and Allen, T. D. (1995) Structural and functional organization of the nuclear envelope. *Curr. Opin. Cell Biol.* **7,** 301–309
61. Yoshihara, T., Omer, E.-L., Koshino, H., Sakamura, S., Kikuta, Y., and Koda, Y. (1989) Structure of a tuber-inducing stimulus from potato leaves (Solanum tuberosum L.). *Agric. Biol. Chem.* **53,** 2835–2837
62. Nakamura, Y., Mithöfer, A., Kombrink, E., Boland, W., Hamamoto, S., Uozumi, N., Tohma, K., and Ueda, M. (2011) 12-Hydroxyjasmonic acid glucoside is a COI1-JAZ-independent activator of leaf-closing movement in samanea saman. *Plant Physiol.* **155,** 1226–1236
63. Bell, E. M., Lin, W. C., Husbands, A. Y., Yu, L., Jaganatha, V., Jablonska, B., Mangeon, A., Neff, M. M., Girke, T., and Springer, P. S. (2012) *Arabidopsis* lateral organ boundaries negatively regulates brassinosteroid accumulation to limit growth in organ boundaries. *Proc. Natl. Acad. Sci. U.S.A.* **109,** 21146–21151
64. Mizutani, M., and Ohta, D. (2010) Diversification of P450 genes during land plant evolution. *Annu. Rev. Plant Biol.* **61,** 291–315
65. Bartel, B., and Fink G. R. (1995) ILR1, an amidohydrolase that releases active indole-3-acetic acid from conjugates. *Science* **268,** 1745–1748
66. Ludwig-Müller, J. (2011) Auxin conjugates: their role for plant development and in the evolution of land plants. *J. Exp. Bot.* **62,** 1757–1773
67. Campanella, J. J., Larko, D., and Smalley, J. (2003) A molecular phylogenomic analysis of the ILR1-like family of IAA amidohydrolase genes. *Comp. Funct. Genomics* **4,** 584–600